A novel role for the Pol I transcription factor UBTF in maintaining genome stability through the regulation of highly transcribed Pol II genes

Elaine Sanij,[1,2,3] Jeannine Diesch,[1,2] Analia Lesmana,[1,2] Gretchen Poortinga,[1,2,4] Nadine Hein,[1,2] Grace Lidgerwood,[1] Donald P. Cameron,[1,2] Jason Ellul,[1,2] Gregory J. Goodall,[5,6,7] Lee H. Wong,[8] Amardeep S. Dhillon,[1,2,3] Nourdine Hamdane,[9,10] Lawrence I. Rothblum,[11] Richard B. Pearson,[1,2,8,12] Izhak Haviv,[3,13,16] Tom Moss,[9,10] and Ross D. Hannan[1,2,8,12,14,15,16]

[1]Research Division, Peter MacCallum Cancer Centre, East Melbourne, Victoria 3002, Australia; [2]Sir Peter MacCallum Department of Oncology, University of Melbourne, Parkville, Victoria 3010, Australia; [3]Department of Pathology, University of Melbourne, Parkville, Victoria 3010, Australia; [4]Department of Medicine, University of Melbourne, Parkville, Victoria 3010, Australia; [5]Centre for Cancer Biology, SA Pathology and University of South Australia, Adelaide, South Australia 5000, Australia; [6]Discipline of Medicine, The University of Adelaide, Adelaide, South Australia 5005, Australia; [7]School of Molecular and Biomedical Science, The University of Adelaide, Adelaide, South Australia 5005, Australia; [8]Department of Biochemistry and Molecular Biology, Monash University, Clayton, Victoria 3800, Australia; [9]Department of Molecular Biology, Medical Biochemistry and Pathology, Faculty of Medicine, Laval University, Québec, QC, G1V 0A6, Canada; [10]St-Patrick Research Group in Basic Oncology, Québec University Hospital Research Centre, Québec, QC, G1R 3S3, Canada; [11]Department of Cell Biology, University of Oklahoma College of Medicine, Oklahoma City, Oklahoma 73104, USA; [12]Department of Biochemistry and Molecular Biology, University of Melbourne, Parkville, Victoria 3010, Australia; [13]Faculty of Medicine, Bar-Ilan University, Zfat, 13100, Israel; [14]Division of Cancer Medicine, Peter MacCallum Cancer Centre, East Melbourne, Victoria 3002, Australia; [15]School of Biomedical Sciences, University of Queensland, Brisbane 4072, Queensland, Australia

Mechanisms to coordinate programs of highly transcribed genes required for cellular homeostasis and growth are unclear. Upstream binding transcription factor (UBTF, also called UBF) is thought to function exclusively in RNA polymerase I (Pol I)-specific transcription of the ribosomal genes. Here, we report that the two isoforms of UBTF (UBTF1/2) are also enriched at highly expressed Pol II-transcribed genes throughout the mouse genome. Further analysis of UBTF1/2 DNA binding in immortalized human epithelial cells and their isogenically matched transformed counterparts reveals an additional repertoire of UBTF1/2-bound genes involved in the regulation of cell cycle checkpoints and DNA damage response. As proof of a functional role for UBTF1/2 in regulating Pol II transcription, we demonstrate that UBTF1/2 is required for recruiting Pol II to the highly transcribed histone gene clusters and for their optimal expression. Intriguingly, lack of UBTF1/2 does not affect chromatin marks or nucleosome density at histone genes. Instead, it results in increased accessibility of the histone promoters and transcribed regions to micrococcal nuclease, implicating UBTF1/2 in mediating DNA accessibility. Unexpectedly, UBTF2, which does not function in Pol I transcription, is sufficient to regulate histone gene expression in the absence of UBTF1. Moreover, depletion of UBTF1/2 and subsequent reduction in histone gene expression is associated with DNA damage and genomic instability independent of Pol I transcription. Thus, we have uncovered a novel role for UBTF1 and UBTF2 in maintaining genome stability through coordinating the expression of highly transcribed Pol I (UBTF1 activity) and Pol II genes (UBTF2 activity).

[Supplemental material is available for this article.]

Transcription of ribosomal RNA (rRNA) genes (rDNA) is mediated by RNA polymerase I (Pol I) and its associated transcription machinery to produce the 45S rRNA precursor of the 28S, 5.8S, and 18S rRNA components of the ribosome (McStay and Grummt 2008). In rapidly growing mammalian cells, rRNA synthesis accounts for 35%–60% of all RNA transcription (Moss and Stefanovsky 2002; Cavanaugh et al. 2003). Accordingly, the Pol I transcription rate is tightly coupled to cellular growth and proliferation rates (Hannan and Rothblum 1995; Moss and Stefanovsky 2002; McStay and Grummt 2008; Chan et al. 2011; Hein et al. 2012; Diesch et al. 2014). We have shown that the consistent up-regulation of rRNA synthesis in cancer cells is necessary for malignant transformation in certain settings (Drygin et al. 2011; Bywater et al. 2012), while small molecule inhibitors of Pol I transcription are currently in

preclinical development and phase I trials for cancer therapy (Hein et al. 2013; Drygin et al. 2014; Poortinga et al. 2014). Despite this, the exact molecular mechanism by which Pol I transcription is coordinated with Pol II transcriptional programs to ensure orderly cellular homeostasis is not fully understood. In this report, we propose a functional role for the Pol I-specific transcription factor UBTF1/2 in coordinating Pol I-mediated rDNA transcription with expression of highly active Pol II-transcribed genes.

UBTF1/2 belongs to the sequence nonspecific class of HMG (high mobility group) proteins. It has six HMG-box homology domains and has been proposed to interact with DNA as a dimer and to induce six in-phase bends to generate a single 360°-loop structure that resembles the nucleosome (Stefanovsky et al. 2001). UBTF1/2 binds across the transcribed and control regions of the rRNA genes (Supplemental Fig 1A; O'Sullivan et al. 2002; Sanij and Hannan 2009), probably explaining its multiple roles in pre-initiation complex (PIC) formation, transcription initiation, and elongation (for review, see Moss et al. 2007; McStay and Grummt 2008; Sanij and Hannan 2009). Indeed, total ablation of *Ubtf1/2* eliminates all rRNA gene transcription and leads to changes in rDNA chromatin (Hamdane et al. 2014).

We have previously shown that UBTF1, but not the naturally occurring splice variant UBTF2, is essential in determining and maintaining the euchromatic state of active rDNA in mammalian cells (Sanij et al. 2008). Further, we have reported that depletion of *Ubtf1/2* by RNA interference (RNAi) silences active rRNA genes and is associated with histone H1-induced assembly of transcriptionally inactive rDNA chromatin (Sanij et al. 2008). Indeed, UBTF1/2 localizes with decondensed active rDNA, while inactive rDNAs appear as bright dense loci devoid of UBTF1/2 (Supplemental Fig. 1B) that are enhanced in number by *Ubtf1/2* loss (Hamdane et al. 2014). This is in agreement with its reported function in establishing and maintaining the undercondensed structure of active nucleolar organizer regions (NORs), which is required for rDNA transcription and nucleolar assembly (Mais et al. 2005; Sanij et al. 2008; Sanij and Hannan 2009; Grob et al. 2014; Hamdane et al. 2014).

Intriguingly, UBTF2 was identified in a functional screen as an enhancer of the beta-catenin pathway (Grueneberg et al. 2003). Further, UBTF1/2 was noted to be putatively enriched at Pol II genes across the human genome (Zentner et al. 2011). However, the role of extra-nucleolar UBTF1/2 is unknown. Indeed, the prevailing consensus in the transcription field is still overwhelmingly that UBTF1/2 is exclusively a Pol I transcription factor (Grob et al. 2014). Here we demonstrate that in addition to the Pol I loci, UBTF1/2 is enriched at and regulates highly expressed Pol II-transcribed genes including histone gene clusters. Further, ChIP-seq analysis of UBTF1/2 binding in tumorigenic human epithelial cells compared to isogenically matched primary cells reveals an additional repertoire of UBTF1/2 target genes involved in regulation of cell cycle checkpoints and DNA damage response. Depletion of *Ubtf1/2* by RNAi leads to DNA damage and genomic instability independent of Pol I transcription. Together, our data demonstrate a novel and unexpected role for UBTF1 and UBTF2 in coordinating Pol I-mediated rDNA transcription with expression of distinct sets of highly active Pol II-transcribed genes that control cell cycle progression and genome integrity.

Results

UBTF1/2 binds highly active Pol II-transcribed genes

To identify a species and cell type-independent core set of UBTF1/2 target genes, we performed ChIP-seq analysis in mouse NIH3T3

cells (post-crisis, immortalized embryonic fibroblasts) and the human primary mammary epithelial cell line (HMEC) immortalized by expressing TERT, the catalytic subunit of telomerase (Elenbaas et al. 2001). We identified, respectively, 3705 and 10,726 genomic regions with significant UBTF1/2 enrichment across the mouse and human genomes, of which, respectively, 46% and 52% overlapped any exon/intron of known RefSeq genes (Fig. 1A,B). In both mouse and human cells, ~40% of all UBTF1/2 binding overlapped with first exons and introns of annotated genes. Indeed, UBTF1/2 enrichment shows preference for binding near transcription start sites (TSSs), whereas no significant binding preference was observed at the transcription termination sites (TTSs) (Fig. 1C). Gene ontology analysis using the Genomic Regions Enrichment of Annotation Tool (GREAT) (McLean et al. 2010) identified chromatin assembly and nucleosome organization and assembly as the biological processes most significantly enriched with UBTF1/2-bound genes and common between the mouse and human data sets (Supplemental Fig. 2A,B). These categories include chromatin remodeling factors and, significantly, a large number of histone genes (Supplemental Tables 1, 2), implicating a role for UBTF1/2 in their transcriptional regulation. To confirm UBTF1/2 enrichments at these non-rDNA loci identified by ChIP-seq, we examined UBTF1/2 DNA binding manually by quantitative ChIP (qChIP) at genes encoding histone genes, chromatin remodeling factors (*Asf1a*, *Smarca5*, and *Dnmt3a*), and also potential UBTF1/2 target genes that did not appear within gene ontological categories, e.g., deoxyuridine triphosphatase (*Dut*), the oncogene *Myc*, and the member of the structural maintenance of chromosome family (*Smc4*) (Fig. 1D). The qChIP data showed significant enrichment in UBTF1/2 at these genes as compared to controls, including the intergenic spacer (IGS) of rDNA that does not bind UBTF1/2 (Fig. 1D).

We intersected the lists of annotated genes bound by UBTF1/2 within ±2 kb of TSSs in the NIH3T3 and HMEC data sets and identified 699 genes that were common between the mouse and human analyses (Fig. 1E; Supplemental Table 14). Gene ontology analysis of the intersected genes showed regulation of gene silencing, chromatin, and nucleosome assembly categories to be the most significantly enriched with UBTF1/2-bound genes (Supplemental Fig. 2C). The gene lists for these ontology terms consisted mainly of histone genes and chromatin remodeling factors (Supplemental Tables 3–5), suggesting a conserved function for UBTF1/2 in their transcriptional regulation. Given that histone genes are among the most highly expressed genes in the human genome (Anamika et al. 2012), we investigated whether UBTF1/2 binding correlates with transcriptional activity. Indeed, a correlation of UBTF1/2 DNA binding with global gene expression in NIH3T3 cells identified genes enriched with UBTF1/2 at their TSSs to be expressed at high levels compared to non-UBTF1/2-bound genes and all genes in the genome (Fig. 1F).

We next examined the enrichments of a variety of post-translational histone modifications, Pol II binding, and DNase I hypersensitivity (HS) profiles at UBTF1/2-bound regions in NIH3T3 cells (Fig. 2A). We observed little correlation between UBTF1/2 binding and the presence of the transcriptional repressive mark H3K9me3. However, almost 50% of the UBTF1/2 peaks overlapped with the activating H3K4me3, H4K9ac, and H4 hyperacetylation marks and Pol II enrichment. Further, almost 70% of UBTF1/2-bound regions are defined as DNase I hypersensitive sites, indicative of open and accessible chromatin (Fig. 2A). Thus, our data strongly suggest specific preference for UBTF1/2 binding to open chromatin structures associated with active promoters and gene bodies.
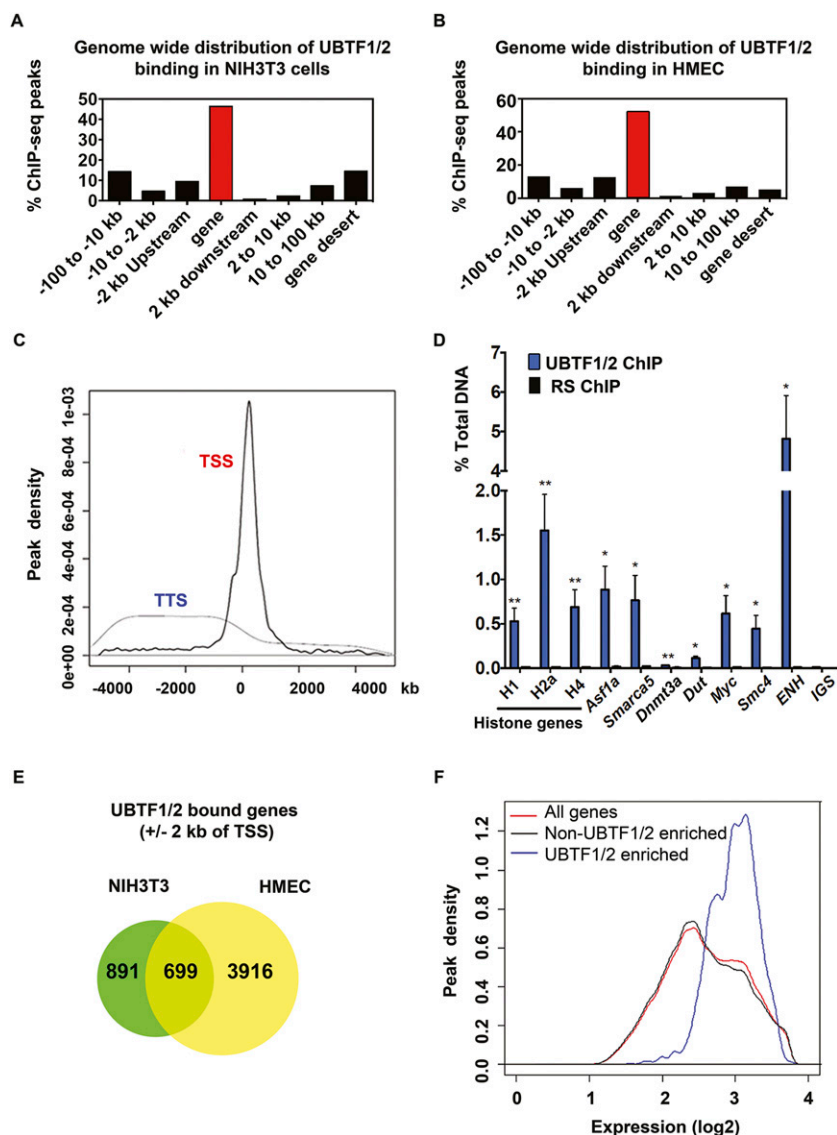
Figure 1. ChIP-seq analysis of UBTF1/2. Distribution of UBTF1/2 binding sites in NIH3T3 (*A*) and HMEC (*B*) with respect to RefSeq genes as determined by Sole-Search. (*C*) Average UBTF1/2 ChIP-seq enrichment profiles at all unique TSSs and TTSs in the mouse genome ± 5 kb. (*D*) qChIP analysis of UBTF1/2 binding in NIH3T3 cells to ChIP-seq genomic regions that reside within the indicated genes. The percentage of DNA immunoprecipitated with anti-UBTF1/2 or rabbit serum (RS) antibodies was calculated relative to the unprecipitated input control (n = 3–7; Ave ± SEM). (*) P-value < 0.05, (**) P-value < 0.01, compared to corresponding RS samples. Amplicons at the enhancer (ENH) and intergenic spacer (IGS) of rDNA were used as a positive and negative control for UBTF1/2 binding, respectively. Primers to core histone genes recognize multiple genes within each class (Supplemental Table 19). (*E*) Venn diagram indicating the overlap of UBTF1/2-bound genes between the NIH3T3 and HMEC cell lines. (*F*) Density histograms of gene expression levels in exponentially growing NIH3T3 cells for all genes, genes with significant UBTF1/2 ChIP-seq peaks < 2 kb from their TSS, or genes with no UBTF1/2 binding at their TSS. Statistical significance between groups was assessed using t-tests.

Interestingly, UBTF1/2 ChIP-seq peaks account for only 1.7% of all DNase I HS regions across the genome (Fig. 2A). This suggests that UBTF1/2 preferentially binds a specific subclass of open highly transcribed chromatin. In order to confirm the specificity of UBTF1/2 binding to DNA, we performed ChIP-seq analysis of POLR1A, the largest subunit of the RNA Pol I complex as both Pol I and UBTF1/2 co-occupy the highly transcribed Pol I-dependent rDNA loci (Supplemental Fig. 1A). We detected 1409 and 9296

peaks of Pol I binding across the mouse and human genomes, some of which we validated manually by qChIP (Supplemental Fig. 3A). However, a comparison of UBTF1/2 and POLR1A ChIP-seq analysis in NIH3T3 and HMEC cell lines revealed little overlap in binding (less than 8% and 3%) across the mouse and human genomes, respectively (Fig. 2B). Thus the data demonstrate that the Pol I transcription apparatus does not simply colocalize indiscriminately at open chromatin and that the enrichment at classes of genes involved in chromatin assembly and nucleosome organization is specific to UBTF1/2. Further, the data strongly suggest that UBTF1/2 does not recruit Pol I to Pol II genes.

Importantly, gene ontology analysis on the intersected UBTF1/2- and Pol II-bound regions revealed negative regulation of megakaryocyte differentiation, chromatin assembly, and regulation of gene silencing to be the biological processes most significantly enriched (Supplemental Fig. 2D). The UBTF1/2-bound gene lists belonging to these ontology terms consisted mainly of chromatin remodeling factors and histone genes (Supplemental Tables 6–9). Thus, our data, collectively along with the known role of UBTF1/2 in regulating rRNA gene transcription, suggest that UBTF1/2 is required for transcription of distinct classes of highly expressed genes involved in cellular proliferative growth, including regulators of chromatin organization.

UBTF1/2 are enriched at a novel subset of Pol II genes in transformed human cells

To determine whether malignant transformation is associated with altered UBTF1/2 enrichment at Pol II genes, we compared UBTF1/2 enrichment in the HMECs (Fig. 1B) to UBTF1/2 enrichment in the tumorigenic HMLER cells, an isogenic HMEC-derived cell line expressing the SV40 large-T, *TERT*, and an oncogenic allele of the *HRAS* gene (expressing HRAS[V12G]) that forms tumors in nude mice (Elenbaas et al. 2001). We identified 11,990 genomic regions with UBTF1/2 enrichment. We next intersected the UBTF1/2 ChIP-seq data in HMECs and HMLERs to identify common and unique regions of UBTF1/2 enrichment in HMLERs (Fig. 2C; Supplemental Fig 2E,F) and identified 3687 UBTF1/2-bound genomic sequences common to both the primary and the tumorigenic cell lines, with genes encoding chromatin and nucleosome assembly being among the most overrepresented (Supplemental Fig. 2E; Supplemental Table 10). Thus the regulation of histone and chromatin remodeling genes is a fundamentally conserved function of
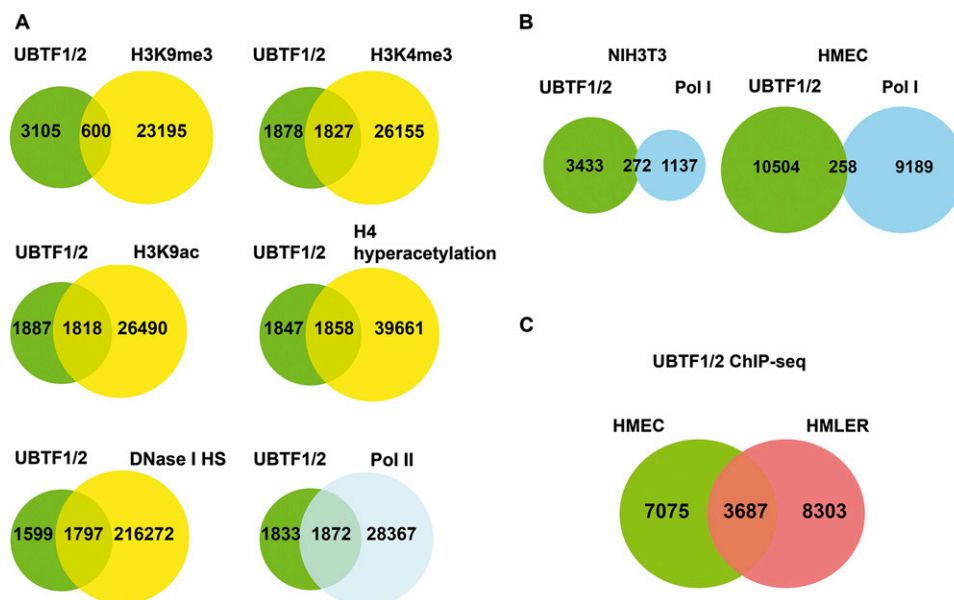
Figure 2. UBTF1/2 binding correlates with markers of open active chromatin. (*A*) Venn diagram indicating overlap of UBTF1/2 binding sites with various chromatin marks, DNase I HS, and Pol II binding in NIH3T3. (*B*) Venn diagram indicating the overlap of UBTF1/2 and Pol I (POLR1A) binding sites in NIH3T3 and HMEC. (*C*) Venn diagram indicating the overlap of UBTF1/2 binding sites between HMEC and HMLER cell lines.

UBTF1/2 in normal and transformed cells. Gene ontology analysis of the UBTF1/2-bound genomic regions unique to the tumorigenic HMLERs revealed biological processes involved in regulating cell cycle checkpoints, DNA damage checkpoints, and DNA damage responses (Supplemental Fig. 2F). Thus, in response to oncogenic transformation, UBTF1/2 targets an additional cohort of target genes whose products include mediators of ATR/ATM-regulated DNA damage response, signal transduction by TP53, and G1 to S transition of the cell cycle (Supplemental Tables 11–13).

Identification of functional occupancy by UBTFI/2 at the histone gene clusters

To determine if UBTF1/2 binding to Pol II regulated genes has a functional effect on gene expression, we performed expression array analysis in control and *Ubtf1/2* depleted NIH3T3 cells using two independent short interfering RNAs (siRNAs) (Supplemental Table 15). We intersected the ChIP-seq and microarray expression

data sets to identify genes whose expression was significantly altered by *Ubtf1/2* knockdown and were bound by UBTF1/2 within 500 bp of their TSSs. Gene ontology analysis, using the MetaCore pathways software (Thomson Reuters), of the biological processes that are enriched in the intersected list identified a significant overrepresentation of genes belonging to chromatin/nucleosome assembly and DNA packaging, including canonical histone genes and histone gene variants, indicating that their transcription may be directly regulated by UBTF1/2 (Table 1). We then chose the histone gene clusters for further functional characterization in examining UBTF1/2's role in mediating Pol II transcription.

The five classes of genes encoding the canonical histone proteins (H2A, H2B, H3, H4, and H1) are arranged in repetitive units in one major and two smaller gene clusters (Marzluff et al. 2002) somewhat reminiscent of the rDNA repeats. Histone mRNAs are transcribed at a high rate as the cells enter S phase in parallel with DNA replication (Marzluff et al. 2008). In addition, there are rep-

Table 1: MetaCore ontology analysis of UBTF1/2-bound genes within 500 bp of their TSSs that are differentially expressed following *Ubtf1/2* knockdown in NIH3T3 cells

Enrichment analysis report

			Common	
Enrichment by GO processes				
#	Processes	Total	*P*-value	In data
1	Chromatin assembly	130	3.185×10^{-13}	14
2	Enzyme-linked receptor protein signaling pathway	820	3.217×10^{-13}	29
3	DNA packaging	176	1.397×10^{-12}	15
4	Chromatin assembly or disassembly	146	1.599×10^{-12}	14
5	Protein-DNA complex assembly	146	1.599×10^{-12}	14
6	Nucleosome assembly	124	3.266×10^{-12}	13
7	Protein-DNA complex subunit organization	154	3.332×10^{-12}	14
8	System development	3997	4.532×10^{-12}	64
9	Multicellular organismal development	4704	7.630×10^{-12}	70
10	DNA conformation changes	205	1.270×10^{-11}	15

Only the most significantly enriched gene ontologies are listed. *P*-value denotes the significance of the number of genes from the intersected list (In data) when compared to the total number of genes in the gene ontology classification (Total).

lication-independent variant histone genes that are not located within the histone gene clusters and are constitutively transcribed throughout the cell cycle. These genes encode histone variants such as H1.0, H2A.Z, H2A.X, H3.3A, and H3.3B, which are known to have distinct functions (Marzluff et al. 2008).

We detected robust peaks of UBTF1/2 enrichment at 33/45 canonical histone genes and 4/6 histone H1 genes within histone cluster 1, 4/10 genes within histone cluster 2 (Fig. 3A,B), and also at the single histone H4 gene located on chromosome 12 in NIH3T3, but none at the small histone cluster 3. In addition, UBTF1/2
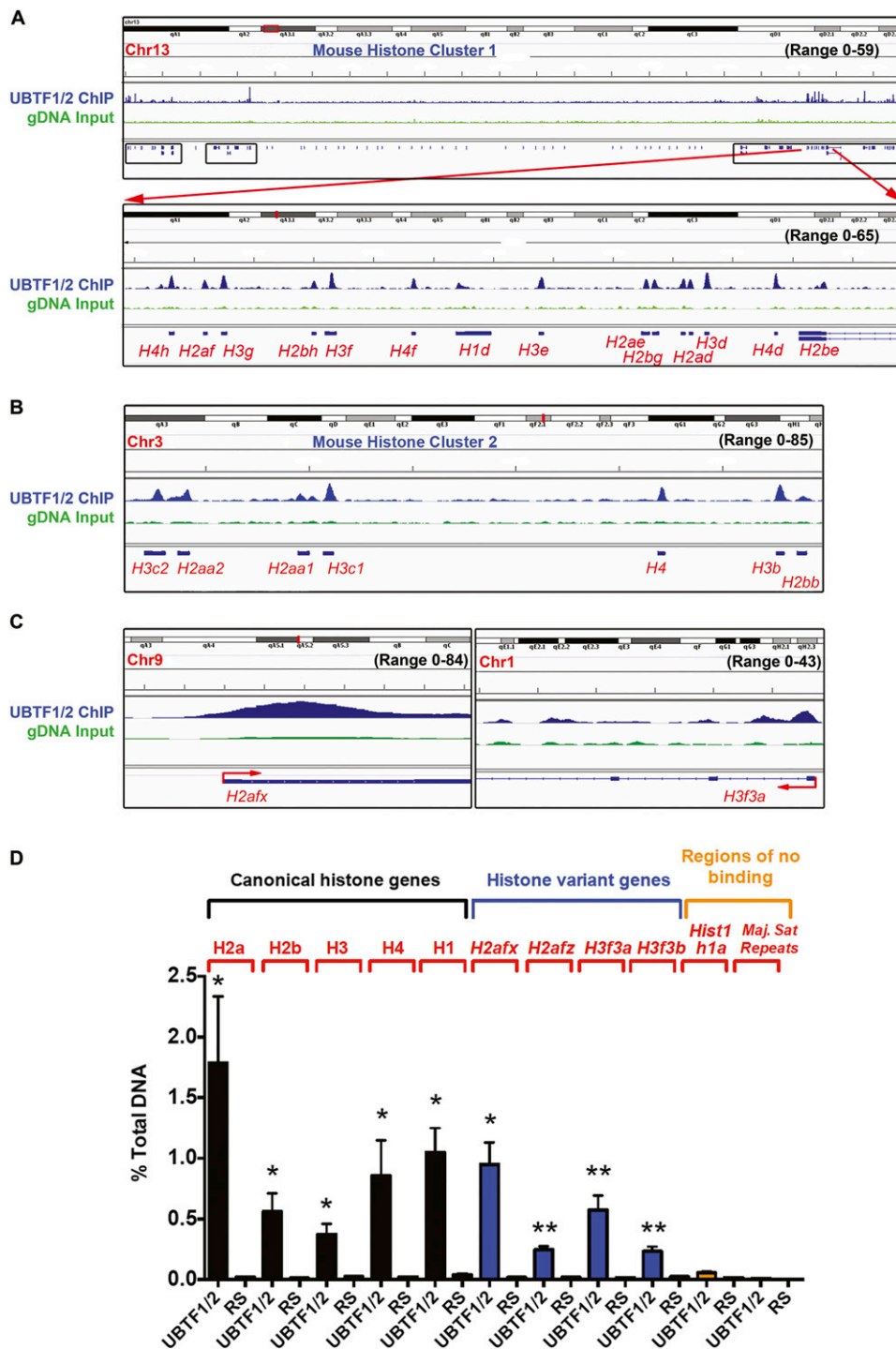

Figure 3. UBTF1/2 binds histone genes. (A–C) IGV (Integrated Genome Viewer) screenshots of mapped reads from UBTF1/2 ChIP and input gDNA at mouse histone gene cluster 1 (A), cluster 2 (B), and histone variant genes *H2afx* and *H3f3a* (C) in NIH3T3 cells. (D) qChIP analysis of UBTF1/2 binding to canonical and variant histone genes in NIH3T3 cells. qChIPs were performed as described in Figure 1D (n = 4; Ave ± SEM). (*) P-value < 0.05, (**) P-value < 0.01, compared to corresponding RS samples. Amplicons at *Hist1h1a* and major satellite repeats were used as a negative control for UBTF1/2 binding.

binding was detected at six histone gene variants, which are dispersed across the genome, including *H2afy, H2afx, H2afz, H3f3a, H3f3b,* and *H1f0* (Fig. 3C). A similar enrichment of UBTF1/2 was observed at histone gene clusters and histone variants in HMEC (Supplemental Fig. 3B,C; Supplemental Tables 16, 17).

Using qChIP, we confirmed significant enrichment of UBTF1/2 binding at the canonical and histone variant genes compared to two regions that ChIP-seq data indicate are not bound by UBTF1/2 (the major satellite repeats and an amplicon specific to *Hist1h1a*) (Fig 3D). These data suggest that histone genes are likely bona fide targets of UBTF1/2.

UBTF1/2 mediates histone gene expression

As *Ubtf1/2* depleted NIH3T3 cells display a delay in G1-S progression (Supplemental Fig. 3D), we examined the effect of *Ubtf1/2* depletion on histone mRNA levels in sorted G1 and S populations from sir*Egfp* control and *Ubtf1/2* knockdown samples to control for any cell cycle bias. Histone H4 and *H2afx* mRNA levels were significantly reduced following *Ubtf1/2* knockdown in the G0/G1 and in the S phase samples (Fig. 4A), suggesting that the decrease in histone mRNA expression is a direct consequence of *Ubtf1/2* knockdown rather than accumulation of cells in G1. Indeed, in the G0/G1 populations, mRNA levels of all canonical and histone variant mRNAs were significantly decreased following *Ubtf1/2* depletion (Fig. 4B). Thus, UBTF1/2 plays a permissive role in mediating mRNA expression of canonical and variant histone genes rather than functioning in the activation of canonical histone gene expression in S phase. Furthermore, consistent with UBTF1/2 regulating mRNA expression of histone genes, transient *Ubtf1/2* knockdown significantly reduced the abundance of histone proteins as represented by H2A and H1 (Supplemental Fig. 4A,B).

UBTF1/2 mediates Pol II recruitment and transcription of histone genes independent of chromatin modifications or nucleosome loading

To examine the mechanism underlying UBTF1/2-mediated regulation of histone gene expression, we performed sequential ChIP assays (ChIP-reChIP) experiments to investigate the overlap between UBTF1/2 and Pol II or Pol I at histone genes. The data showed that UBTF1/2 and Pol II simultaneously occupy histone genes (Supplemental Fig. 4C). Consistent with the lack of overlap observed in UBTF1/2 and Pol I binding across the genome (Fig. 2B), we observed no enrichment in Pol I occupancy at histone genes (Fig. 4C; Supplemental Fig. 4C). This eliminates the possibility of UBTF1/2 recruiting Pol I to histone gene loci.

To confirm that UBTF1/2 directly regulates transcription of histone genes via Pol II, we examined Pol II recruitment to histone genes in response to modulation of UBTF1/2 levels. To a large extent, the phosphorylation status of the C-terminal domain (CTD) of the largest subunit of Pol II defines the stage of transcription (Phatnani and Greenleaf 2006). Pol II is recruited into the PIC with a hypophosphorylated CTD; the CTD is phosphorylated on Serine 5 (Ser5) during initiation and promoter clearance and then on Serine 2 (Ser2) during elongation (Fuda et al. 2009). We observed significant reductions in total Pol II and Pol II (Ser5) loading at histone H2a, H4, and H1 genes in *Ubtf1/2* depleted cells (Fig. 4C), suggesting that UBTF1/2 is required for recruitment and initiation of Pol II transcription at histone genes. Interestingly, we also observed proportionally greater reduced occupancy of elongating Pol II (Ser2) at histone genes compared to the observed reduction in

Pol II loading/initiation following *Ubtf1/2* knockdown. This suggests a role for UBTF1/2 in mediating Pol II elongation rates, consistent with its ability to mediate Pol I elongation (Stefanovsky et al. 2006).

Ubtf1/2 knockdown did not correlate with any significant changes in chromatin modifications at histone H2a and H1 genes (Supplemental Fig. 4D), indicating that UBTF1/2's role in regulating histone gene expression is downstream or independent of the establishment of the euchromatic environment within the histone gene clusters. Furthermore, we did not observe significant changes in the enrichment of histones H3, H4, or linker histone H1 loading at histone H2a and H1 genes following *Ubtf1/2* knockdown (Supplemental Fig. 4D). Thus, UBTF1/2 does not alter nucleosome loading at histone genes. To further examine the effect of UBTF1/2 binding on chromatin remodeling events at histone genes, we designed primers tiling the 340-bp region that spans the promoter, the TSS, and the transcribed region of *Hist1h2ad* and performed qChIP (Fig. 4D). UBTF1/2 binding at *Hist1h2ad* was ~10- to 15-fold higher at amplicons within the transcribed region compared to the promoter (Fig. 4E). We then examined nucleosome positioning at *Hist1h2ad* by chromatin accessibility assay (CHART-PCR) (Rao et al. 2001). Micrococcal nuclease (MNase) accessibility measurements of control samples revealed the region spanning −194 to +15 bp of *Hist1h2ad* (amplicons P-1, P-2, and A) is highly sensitive to MNase digestion compared to the transcribed region (+32 to +144 bp, amplicons B and C) (Fig. 4F), suggesting that it is depleted of a nucleosome as expected for a highly constitutively transcribed gene. Despite the fact that histone genes are present within an open chromatin context (Hovhannisyan et al. 2003; Medina et al. 2012), *Ubtf1/2* knockdown led to a significant decrease in protection against MNase digestion at the promoter and also at the transcribed region (Fig. 4F). This suggests that UBTF1/2 interacts directly with DNA as opposed to nucleosomes and its binding modulates DNA accessibility to promote Pol II binding independent of nucleosome occupancy. The data further suggest that UBTF1/2-wrapped chromatin (Stefanovsky et al. 2001) is a preferred template for Pol II rather than histone-wrapped chromatin.

UBTF2 is required for optimal histone gene expression

UBTF2 is inactive in regulating rDNA transcription compared with UBTF1 (Grummt 1999; Hannan et al. 1999; Stefanovsky and Moss 2008) and does not function in remodeling chromatin at the rDNA repeats in the absence of UBTF1 (Sanij et al. 2008). To address the relative contribution of UBTF1 and UBTF2 isoforms to Pol II histone gene expression, we performed replacement experiments with rat FLAG-*Ubtf1* and FLAG-*Ubtf2* cDNAs, which contain nucleic acid sequence differences in the region targeted by the murine-specific sir*Ubtf1/2* (Supplemental Fig. 5A; Sanij et al. 2008), and performed qChIP assays using anti-FLAG antibodies. We found that both FLAG-rUBTF1 and FLAG-rUBTF2 can interact with histone genes independently of endogenous UBTF1 and UBTF2 (Supplemental Fig. 5B). Next, we performed RNAi knockdown targeting *Ubtf1* and *Ubtf2* mRNAs or only *Ubtf1* mRNA (we are unable to selectively target *Ubtf2* by RNAi) (Fig. 5A). While total UBTF1/2 enrichment was significantly reduced at histone genes in *Ubtf1/2* depleted cells, *Ubtf1* knockdown cells exhibited similar enrichment of total UBTF1/2 loading to control cells, indicating that UBTF2 is able to fully occupy histone genes independently of UBTF1 (Fig. 5B). Moreover, while *Ubtf1/2* knockdown significantly reduced histone H2a, H1, and H4 mRNA levels, *Ubtf1* knockdown failed to reduce histone mRNA levels, demonstrating that UBTF2 is
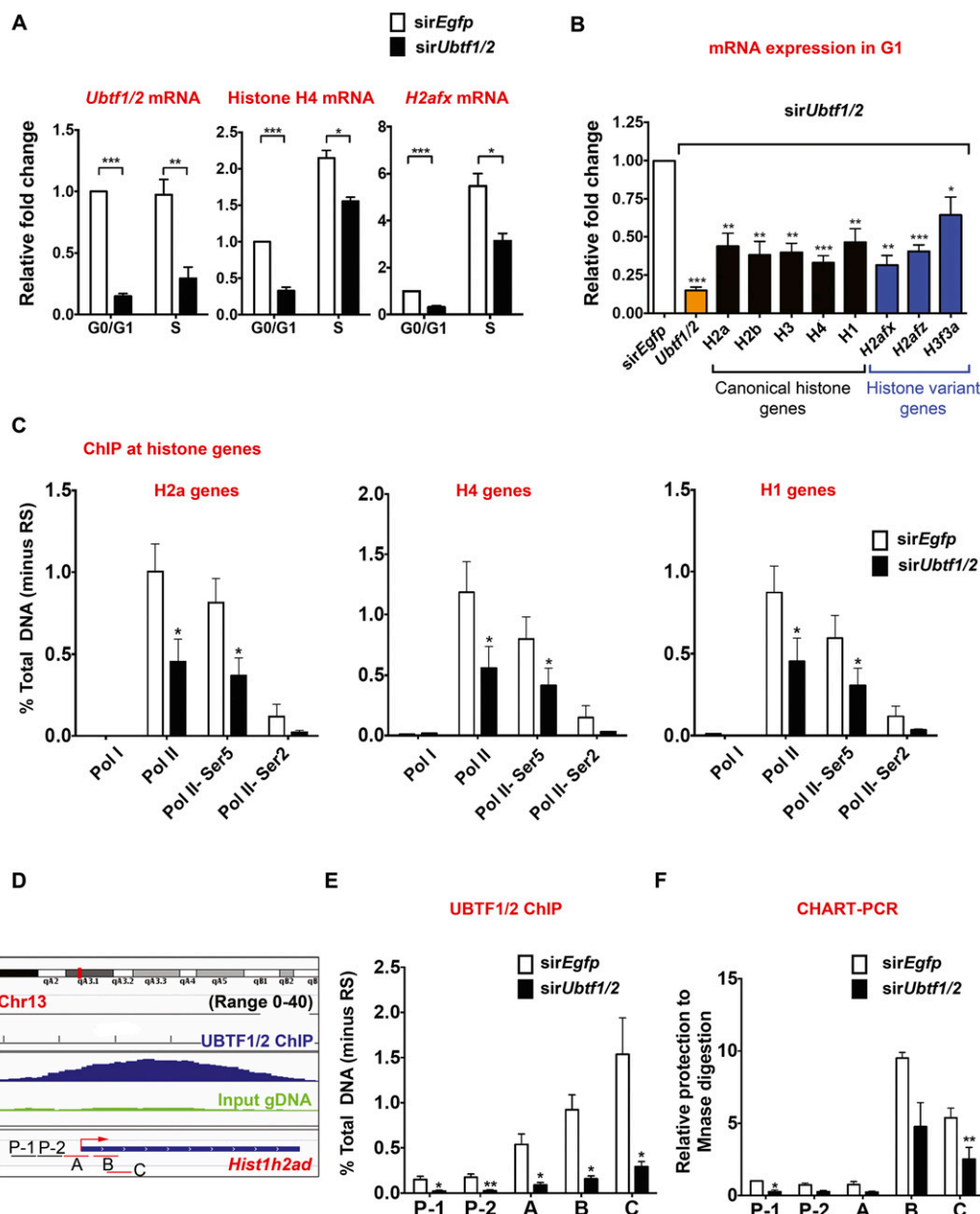
Figure 4. UBTF1/2 regulates histone gene expression by mediating Pol II recruitment. (*A*) NIH3T3 cells were transfected with sir*Egfp* or sir*Ubtf1/2*#1 for 48 h, then collected and incubated with Vybrant DyeCycle Violet stain (Life Technologies). Cells were then analyzed using BD FACSAria, and G1 and S phase populations were sorted based on DNA content. Total RNA was extracted and *Ubtf1/2*, Histone H4, and *H2afx* mRNA levels were determined by reverse transcription qPCR. mRNA levels were normalized to beta-2-microglobulin (*B2m*) mRNA and expressed as fold change relative to sir*Egfp*/G0/G1 (*n* = 4). (*B*) Total RNA samples from G1 population of NIH3T3 cells transfected with sir*Egfp* or sir*Ubtf1/2*#1 as in *A* were analyzed by reverse transcription qPCR for mRNA expression of various canonical and variant histone genes as indicated (*n* = 4). (*C*) UBTF1/2 mediates Pol II recruitment, initiation, and elongation at histone genes. qChIP analysis of the histone H2a, H4, and H1 genes in sir*Egfp*- or sir*Ubtf1/2*#1-transfected NIH3T3 cells using antibodies against Pol I (*n* = 2), total Pol II (*n* = 7), phospho Pol II-Ser5 (*n* = 4), or phospho Pol II-Ser2 (*n* = 4). The percentage of DNA immunoprecipitated with the indicated antibodies or RS was calculated relative to the unprecipitated input control. Percentage of DNA of RS controls was subtracted. (*D*) *Ubtf1/2* knockdown leads to increased DNA accessibility at *Hist1h2ad*. Screenshots of IGV with the mapped reads from UBTF1/2 ChIP and input gDNA in NIH3T3 to *Hist1h2ad*. Primers used for qPCR are indicated (Supplemental Table 21). (*E*) qChIP analysis of UBTF1/2 binding at *Hist1h2ad* in sir*Egfp* or sir*Ubtf1/2*#1 transfected NIH3T3 cells. qChIPs were performed as described in Figure 4C (*n* = 3). (*F*) Chromatin remodeling of the *Hist1h2ad* by UBTF1/2. Nuclei from NIH3T3 cells transfected with either sir*Egfp* or sir*Ubtf1/2*#1 for 48 h were incubated with or without MNase. Extracted gDNA was subjected to qPCR using primers outlined in *D*. MNase accessibility was expressed as a percentage of undigested gDNA samples (*n* = 3). In all graphs (*A–F*), error bars represent Ave ± SEM, (*) *P*-value < 0.05, (**) *P*-value < 0.01, (***) *P*-value < 0.001, compared to corresponding sir*Egfp* samples.

sufficient to regulate histone gene expression in the absence of UBTF1 (Fig. 5B). In direct contrast, at the rDNA loci both *Ubtf1/2* and *Ubtf1* knockdown led to a similar 50% reduction in 45S rRNA

levels (Fig. 5A). Thus, although UBTF2 is known to be inactive in Pol I transcription (Grummt 1999; Hannan et al. 1999; Stefanovsky and Moss 2008) and chromatin remodeling at rDNA (Sanij et al.
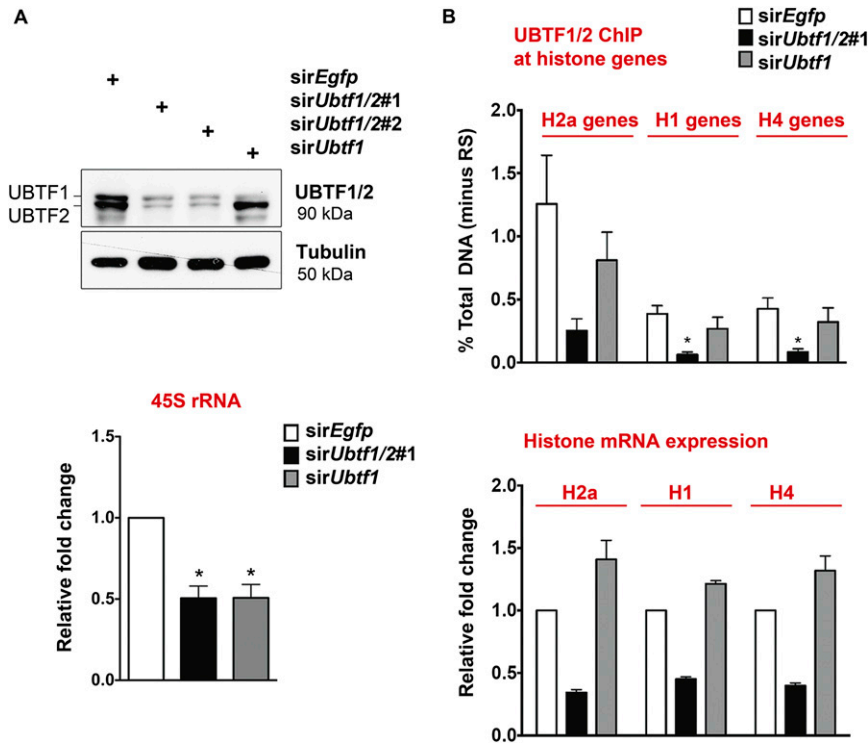
Figure 5. The UBTF2 isoform mediates histone gene expression. (*A*) Total protein lysates from NIH3T3 cells transfected with sir*Egfp*, sir*Ubtf1/2*#1, sir*Ubtf1/2*#2, or sir*Ubtf1* for 48 h were analyzed by Western blotting (*top* panel). RNA was also extracted and 45S rRNA precursor levels were determined by reverse transcription qPCR using primers to the 5′ external transcribed region (ETS) (Supplemental Table 20). 45S rRNA levels were normalized to *Gapdh* mRNA and expressed as fold change relative to sir*Egfp* control (*n* = 3; Ave ± SEM). (*) *P*-value < 0.05 (*bottom* panel). (*B*) (*Top* panel) qChIP analysis of UBTF1/2 binding to histone H2a, H1, and H4 genes in NIH3T3 cells transfected with either sir*Egfp*, sir*Ubtf1/2*#1, or sir*Ubtf1* for 48 h (*n* = 3; Ave ± SEM). (*) *P*-value < 0.05 compared to sir*Egfp* sample. qChIPs were performed as described in Figure 4C. (*Bottom* panel) G1 populations of NIH3T3 cells transfected as above were sorted as described in Figure 4A, and total RNA was extracted. Histone H2a, H1, and H4 mRNA levels were determined by reverse transcription qPCR. mRNA levels were normalized to *B2m* mRNA and expressed as fold change relative to the sir*Egfp* control (*n* = 4; Ave ± SEM). (*) *P*-value < 0.05 relative to corresponding sir*Egfp* samples.

2008), these data demonstrate that UBTF2 functions to enhance Pol II gene expression.

Ubtf1/2 knockdown leads to DNA damage and genomic instability

In eukaryotes, DNA damage and repair occurs in the context of chromatin and thus histone availability affects genome integrity and stability (Ye et al. 2003; Gunjan et al. 2005). Thus, the loss of histone gene expression following *Ubtf1/2* depletion might be associated with DNA damage and/or genome instability. To investigate this possibility, we used the comet assay to detect DNA damage at the single-cell level and found that *Ubtf1/2* knockdown cells exhibited significantly longer comet tails than those of control cells, indicating that they accumulated DNA damage (Fig. 6A).

The appearance of micronuclei is another characteristic marker of damaged chromosomes. Micronuclei are small nuclei separated from the main nucleus, containing chromosomes or chromosome fragments derived from mitotic spindle dysfunction (Fenech 2006). We performed a cytokinesis-block micronucleus (CBMN) assay to quantify micronuclei appearing after a single complete nuclear division. *Ubtf1/2* knockdown cells displayed

a significant increase in binucleated cells exhibiting micronuclei formation (Fig. 6B, D). To examine whether the micronucleus phenotype observed following *Ubtf1/2* depletion was simply caused by reductions in rDNA transcription and its subsequent consequences on nucleolar structure or function, independent of possible effects on Pol II transcription, we performed the CBMN assay following RNAi depletion of the Pol I-specific transcription factor *Rrn3* (Fig. 6C,D). RRN3 has no known functions outside nucleolar rDNA transcription. Knocking down *Ubtf1/2*, *Ubtf1*, or *Rrn3* has similar consequences in reducing 45S rRNA levels (Figs. 5A, 6C). However, while knockdown of *Ubtf1/2* led to a significant increase in micronuclei, *Rrn3* knockdown, and thus selective inhibition of rDNA transcription, failed to increase micronuclei numbers. Moreover, *Ubtf1* knockdown only modestly increased the percentage of cells exhibiting micronuclei, consistent with the proposed model that UBTF2 plays a prominent role in regulating histone genes and other Pol II-transcribed genes. These data reveal that the genomic instability following *Ubtf1/2* knockdown is independent of its effects on rDNA transcription per se and is likely to be a direct consequence of reductions in Pol II gene expression, in particular, histone genes. Further, immunofluorescence for UBTF1/2 combined with rDNA FISH analysis demonstrated that the micronuclei associated with *Ubtf1/2* knockdown did not overlap with the rDNA signal, indicating that genomic material in these micronuclei are not solely derived from rDNA-bearing chromosomes (Supplemental Fig. 6) and do not merely reflect genomic instability of the rDNA repeats but rather genome-wide chromosome instability.

Discussion

UBTF1/2 couples the regulation of a subset of highly transcribed Pol I and Pol II genes

In this study we demonstrate a fundamental role for the Pol I transcription factor UBTF1/2 in regulating highly transcribed Pol II genes, including the histone gene clusters. Moreover, in transformed cells, we demonstrate that UBTF1/2 is enriched at an additional cohort of genes involved in DNA damage and repair, including mediators of ATR/ATM-regulated DNA damage response, signal transduction by TP53, and G1 to S transition of the cell cycle. Activation of the ATM/ATR-regulated DNA damage network following oncogenic stress is proposed to be a biological response to delay or protect against cancer (Bartkova et al. 2005) by pausing cells in S phase or G2 to allow appropriate repair of damaged DNA. It is tempting to speculate that this additional cohort of UBTF1/2 target genes represents a regulated response to oncogenic stress to couple the rate of rDNA transcription with DNA integrity and fidelity of chromatin assembly.

Thus collectively, the data indicate that UBTF1/2 binding is dynamic, context dependent, and potentially associated with
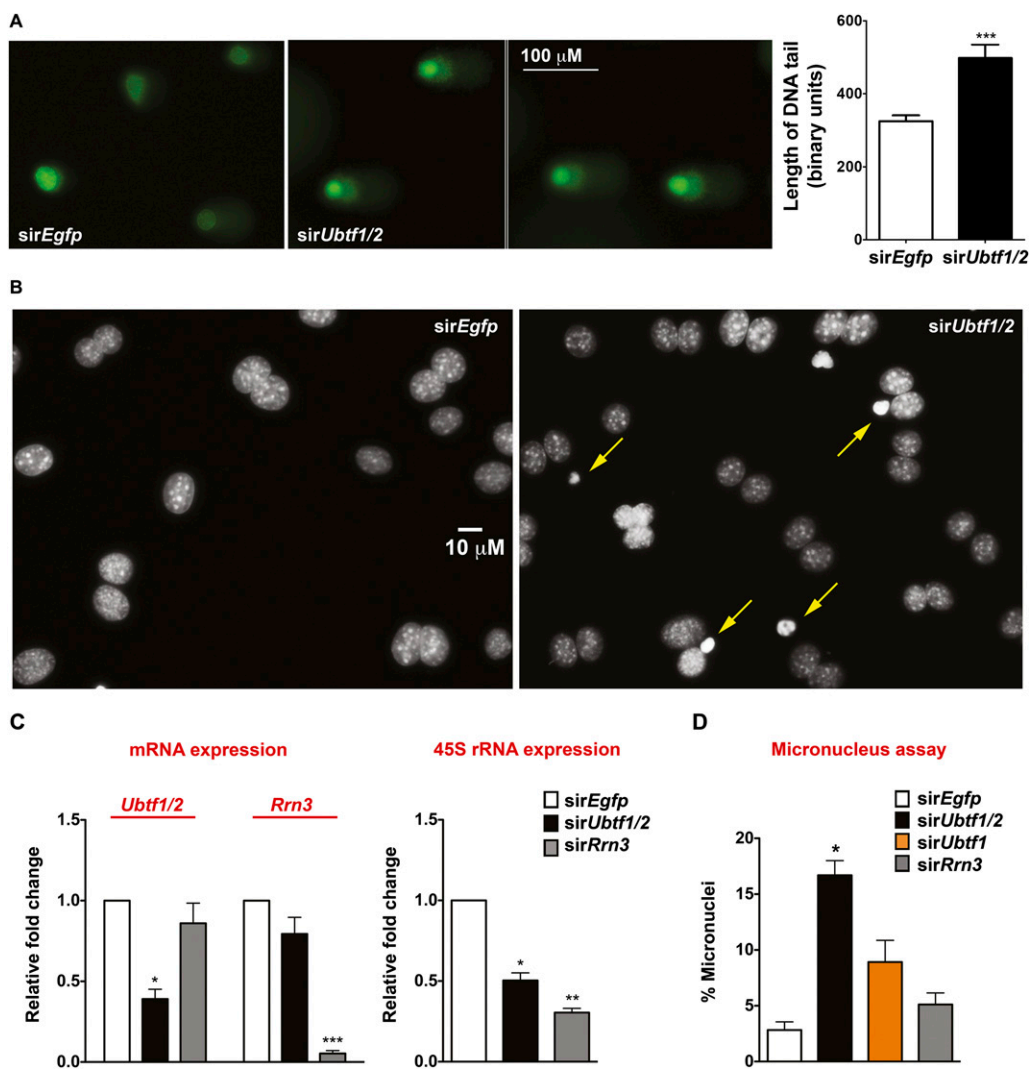
Figure 6. *Ubtf1/2* knockdown leads to DNA damage and genomic instability. (*A*) NIH3T3 cells were transfected with sir*Egfp* or sir*Ubtf1/2*#1 for 48 h and DNA damage was measured by comet assay. Representative images of SYBR green-stained DNA of sir*Egfp* control cells, showing undamaged and supercoiled DNA remaining within the nuclear membrane, while in sir*Ubtf1/2*#1 cells, denatured DNA fragments migrate out from the nucleus in a comet tail. The tail length for ~50 nuclei for each sample from two independent experiments was measured using metamorph software. The graph on the *right* panel represents Ave ± SEM. (*) *P*-value < 0.05 compared to sir*Egfp* control. (*B*) *Ubtf1/2* knockdown leads to abnormal mitosis as measured by the CBMN assay. NIH3T3 cells transfected with sir*Egfp* or sir*Ubtf1/2*#1 were incubated for 24 h, then Cytochalasin B, an inhibitor of cytokinesis, was added at 3 μg/mL for a further 24 h. DAPI staining was then performed and percentages of binucleated cells exhibiting micronuclei were scored (yellow arrows) (*n* = 3; Ave ± SEM). (*) *P* < 0.05. (*C*) Forty-eight hours after transfecting NIH3T3 cells with sir*Egfp*, sir*Ubtf1/2*#1, or sir*Rrn3*, total RNA was extracted, and *Ubtf1/2* mRNA, *Rrn3* mRNA, and 45S rRNA precursor levels were determined by reverse transcription qPCR. mRNA levels were normalized to *B2m* mRNA and expressed as fold change relative to the sir*Egfp* control (*n* = 3; Ave ± SEM). (*) *P*-value < 0.05, (**) *P*-value < 0.01, (***) *P*-value < 0.001, compared to corresponding sir*Egfp* controls. (*D*) NIH3T3 cells were transfected with siRNA oligos as indicated, and the CBMN assay was performed as described in *B* (*n* = 3). Approximately 100 cells were counted in each experiment and percentages of binucleated cells exhibiting micronuclei were scored (Ave ± SEM). (*) *P*-value < 0.05 compared to sir*Egfp* control.

malignant transformation. While a number of Pol II transcription factors have been implicated in the regulation of Pol I, for example, MYC, TP53, and RUNX2 (Hannan et al. 2013), our data provide the first specific in vivo example of a Pol I factor with dual functions in the regulation of Pol I and Pol II.

Interestingly, although ribosomal protein (RP) encoding genes, like histone genes, are also highly expressed genes (Castillo-Davis et al. 2002), they did not appear in the gene ontological analysis of genes bound by UBTF1/2 in NIH3T3 (Supplemental Fig. 2A) nor did they change in mRNA levels upon *Ubtf1/2* knockdown (Supplemental Table 15). In fact, UBTF1/2 ChIP-seq peaks in NIH3T3 cells were detected at only five RP genes. Thus,

the data do not support a model in which ribosome biogenesis is coordinated at the transcriptional level by UBTF1/2. Instead, it is consistent with the prevailing view that in mammals, the major mode of coordinated regulation of ribosome biogenesis is achieved post-transcriptionally via specific conserved signaling networks including the PI3K/AKT/TOR and ERK pathways (White 2008; Chan et al. 2011; Hannan et al. 2011, 2013; Bywater et al. 2013; Chauvin et al. 2014). This appears in contrast to lower organisms such as yeast where transcription of the rRNAs by Pol I and the RPs by Pol II is coordinated (Laferte et al. 2006; Berger et al. 2007). We note that in higher eukaryotes, RPs have evolved extra-ribosomal functions, for example, in regulating nucleolar stress and TP53

accumulation through the binding of certain RPs to MDM2 (Boulon et al. 2010; Deisenroth and Zhang 2010; Hein et al. 2013). The transcriptional uncoupling of rRNA and RP synthesis in higher eukaryotes may allow for regulation of the extra-ribosomal functions of RPs by mechanisms and signaling pathways independent of those that modulate ribosome biogenesis.

Ubtf1/2 are splice variants from a single transcript and their expression is dynamically regulated by >90% during terminal differentiation and proliferation, which coincides with dramatic changes in the rDNA transcription rate (Larson et al. 1993; Moss and Stefanovsky 2002; Sanij et al. 2008; Sanij and Hannan 2009; Poortinga et al. 2011, 2014; Bywater et al. 2012). Conversely, they are robustly up-regulated under proliferative conditions (Moss and Stefanovsky 2002; Sanij and Hannan 2009; Bywater et al. 2012; Poortinga et al. 2014). Critically, our previous studies demonstrated that UBTF2 does not function in Pol I transcription, raising the perplexing question about the UBTF2 function in vivo (Sanij et al. 2008). In this study we demonstrated that UBTF2 is sufficient in the absence of UBTF1 to modulate Pol II gene expression. Moreover, depletion of *Ubtf1* alone had little effect on Pol II-dependent transcription of the histone genes but robustly repressed Pol I-dependent transcription of the rDNA (Fig. 5). Together, these data suggest that UBTF1 functions predominantly in regulating Pol I, while UBTF2 functions in regulating Pol II. Alternative splicing for the same gene to yield two distinct mRNA isoforms, with specific roles in regulating Pol I (*Ubtf1*) and Pol II (*Ubtf2*) transcription, respectively, appears to be an ideal evolutionary mechanism to couple the regulation of highly transcribed genes required for fundamental processes such as rRNA synthesis and chromatin assembly.

Recruitment of UBTF1/2 to open chromatin

The interphase genome is organized into self-interacting topological domains flanked by boundaries. These regions are remodeled by Pol II and topoisomerase activities creating supercoiling domains. Underwound, negatively supercoiled domains are transcriptionally active, enriched in "open" chromatin fibers, DNase I hypersensitive sites, and TSSs (Naughton et al. 2013) reminiscent of chromatin structures bound by UBTF1/2 (Figs. 1C,F, 2A). Like other HMG proteins, UBTF1/2 has little intrinsic DNA binding specificity in vitro. One possibility is that UBTF1/2 may recognize specific topological features that are characteristic of specific DNA regions with very high constitutive transcriptional activity. Indeed, intersection of UBTF1/2-bound regions with DNA supercoiling data across seven genomic loci that distinguish between negative supercoiled "underwound" and positively supercoiled "overwound" DNA (Naughton et al. 2013) demonstrates that ~83% of the overlapping regions represent underwound DNA (data not shown). Thus, UBTF1/2 may "mark" and stabilize regions of constitutively active "underwound" DNA structures. In turn, this may facilitate rapid induction of mRNA synthesis during the cell cycle or in response to extracellular stimuli.

UBTF1/2 as a mediator of genomic stability

UBTF1/2 deficiency, but not reductions in Pol I transcription per se, resulted in genome-wide instability in NIH3T3 cells (Fig. 6). Almost certainly the role UBTF1/2 plays in maintaining high levels of canonical and noncanonical histones and other genes involved in chromatin assembly and DNA damage response contributes to the genomic instability upon *Ubtf1/2* knockdown. This would be consistent with the observations that histone insufficiency during S phase results in spontaneous DNA damage and genomic instability (Han

et al. 1987; Myung et al. 2003; Ye et al. 2003; Prado and Aguilera 2005; Clemente-Ruiz and Prado 2009) and that manipulation of core histone function or abundance causes defects in chromosome segregation (Meeks-Wagner and Hartwell 1986; Pinto and Winston 2000).

Thus, through its ability to coordinately regulate the expression of some of the most highly transcribed Pol I and Pol II genes in the genome including the histones clusters and rDNA repeats, our data demonstrate a previously unrecognized but fundamental role for the two isoforms of UBTF1/2 in coupling Pol I transcription and the cell's capacity to grow with the fidelity of chromatin assembly and DNA repair. Intriguingly, it has recently been demonstrated that inhibition of Pol I is an effective mechanism to treat hematological cancers with drugs targeting Pol I transcription now in clinical trials (Bywater et al. 2012, 2013). We propose that the unique characteristics of UBTF1/2 to target a subset of Pol II genes critical for cell proliferation, in addition to Pol I, make it a highly attractive target for cancer therapy.

Methods

ChIP and ChIP-seq analysis

Standard ChIP was carried out as described (Poortinga et al. 2004; Sanij et al. 2008). Antibodies and primer sequences are listed in the Supplemental Data. ChIP-reChIP experiments were carried out as described in Mendoza-Parra (2012). Anti-UBTF1/2 sera were cross-linked to protein A beads using disuccinimidyl suberate. UBTF1/2 ChIP products were eluted in 1%SDS, 0.1 M NaHCO$_3$, diluted 1:10 and subjected to a second ChIP using antibodies directed against Pol I, Pol II, or RS.

For ChIP-seq of UBTF1/2 ChIP DNA and input gDNA from NIH3T3, libraries from two biological replicates were prepared for the Illumina Genome Analyzer II platform at Peter MacCallum Cancer Center. ChIP-seq libraries of histone modifications and Pol II in NIH3T3 libraries were also prepared for the Illumina Genome Analyzer II platform. Sequencing reads were mapped to the mouse genome database mm9 using the Burrows-Wheeler Aligner (BWA) (Li and Durbin 2009). ChIP-seq of UBTF1/2 ChIP, Pol I, and gDNA samples in HMEC was performed using the Illumina Genome Analyzer II platform, while ChIP-seq of UBTF1/2 ChIP and gDNA samples in HMLER cells was performed using Illumina HiSeq 1000. Sequences were mapped to the human genome (hg19). MACS 1.4 (Model-based Analysis of ChIP-seq [Zhang et al. 2008]) was used to call peaks over input DNA, and the fold enrichment for each peak was calculated using the R package (Gentleman et al. 2004). Only peak regions with a false discovery rate (FDR) <10% and *P*-value < 0.00001 were selected and annotated with RefSeq annotation using the R package ChIPpeakAnno (Zhu et al. 2009). The distribution of UBTF1/2 peaks relative to RefSeq genes as well as the comparison of ChIP-seq data sets was performed using the Sole-Search software tool (Blahnik et al. 2010). The DNase I hypersensitivity profile in NIH3T3 cells was obtained from the ENCODE UCSC Genome Browser (https://www.encodeproject.org/, Accession: ENCSR000CNS).

Gene expression analysis

We performed microarray analysis (Affymetrix, Mouse Exon ST 1.0 arrays) on three biological replicates of *Ubtf1/2* knockdown samples using two independent siRNA oligos, a nonsilencing sir*Egfp* or mock-transfected NIH3T3 samples (Supplemental Table 18). The arrays were normalized using the robust multiarray average expression measure (RMA) (Irizarry et al. 2003), and differential expression was then determined using a linear model and the Limma package (http://bioinf.wehi.edu.au/limma/) (Smyth 2005). Moderated *t*-statistics were generated and signifi-

cance was assessed using the log-fold change and FDR-adjusted *P*-value.

Correlation analysis of UBTFI/2 ChIP-seq and microarray expression data

Expression data of exponentially growing NIH3T3 were obtained using Affymetrix, Mouse Exon ST 1.0 arrays (mock samples from previous section). Triplicates were normalized using the RMA method (Irizarry et al. 2003) and expression values for all genes, genes with significant UBTF1/2 peaks < 2 kb from their TSS, or genes with no UBTF1/2 binding at their TSS, were obtained. Statistical significance between the groups was assessed using *t*-tests.

Cell culture, siRNA knockdown, and RNA expression analysis

NIH3T3 cells were cultured in Dulbecco's modified Eagle's medium (DMEM) with 10% fetal bovine serum (FBS) at 37°C. HMECs and HMLER cells were cultured in HuMEC ready medium (12752010, Life Technologies). Dharmafect 2 reagent (Dharmacon) was used to transfect siRNA at 40 nM. The tetracycline-regulated rat *Ubtf1* and *Ubtf2* MEF-3T3 cell lines were established as reported in Sanij et al. (2008). Cells were lysed, RNA was extracted, and first-strand cDNA was synthesized using random hexamer primers and Superscript III (Invitrogen). Quantitative PCR (qPCR) was performed in duplicate using the FAST SYBR Green dye on the StepOnePlus real-time PCR system (Applied Biosystems). Primer sequences are listed in (Supplemental Table 20).

Western blotting and immunofluorescence

Twenty to fifty milligrams of whole-cell lysates were resolved by SDS-PAGE, electrophoretically transferred onto PVDF membranes (Millipore), and analyzed using enhanced chemiluminescence (ECL) detection (GE Healthcare). For IF, cells were fixed in 4% paraformaldehyde (10 min at room temperature), washed with PBS, and blocked with 5% skim milk powder, 0.5% chicken serum in PBS, and 0.3% Triton X-100 for 30 min. Cells were sequentially incubated with anti-UBTF1/2 sera and Alexa Fluor 594 anti-rabbit secondary antibody (Molecular Probes). Stained cells were fixed again with 4% formaldehyde and counterstained with DAPI in Vectashield mounting media (Vector Labs). Images were acquired on an Olympus BX-51 microscope equipped with a Spot RT camera (model 25.4), using the UPlanAPO 40×, NA 1.2 water immersion objective and the Spot Advanced software, version 4.6.4.3. Settings for adjusting the image after acquisition (i.e., gamma adjust and background subtract settings) were identical for all images. A detailed FISH protocol is provided in the Supplemental Methods.

COMET assay

Cells were collected and processed as described in the manufacturer's protocol (Trevigen, Comet Assay 4250-050-K). Images were acquired on an Olympus BX-51 microscope using the Olympus UPlanAPO 20×, NA 1.2 water immersion objective as described above. Quantitation was performed using MetaMorph (Molecular Devices).

CHART-PCR assay

Cells were collected and mononucleosome preparations were performed using an EpiScope nucleosome preparation kit (#5333; Takara). Briefly, nuclei were isolated from control and *Ubtf1/2* depleted cells and incubated at 37°C for 30 min with MNase. A control without MNase was included for each sample. gDNA was then isolated and subjected to qPCR using FAST SYBR Green dye on the StepOnePlus real-time PCR system (Applied Biosystems).

The relative level of MNase resistance was calculated after normalization to mock-digested DNA.

Data access

Raw ChIP-seq data is available through the NCBI Sequence Read Archive (SRA, http://www.ncbi.nlm.nih.gov/sra/) under accession number SRP039369. Processed ChIP-seq data and microarray expression data have been submitted to the NCBI Gene Expression Omnibus (GEO, http://www.ncbi.nlm.nih.gov/geo/) under accession numbers GSE63255 and GSE55461, respectively.

References

Anamika K, Gyenis A, Poidevin L, Poch O, Tora L. 2012. RNA polymerase II pausing downstream of core histone genes is different from genes producing polyadenylated transcripts. *PLoS ONE* **7:** e38769.

Bartkova J, Horejsi Z, Koed K, Kramer A, Tort F, Zieger K, Guldberg P, Sehested M, Nesland JM, Lukas C, et al. 2005. DNA damage response as a candidate anti-cancer barrier in early human tumorigenesis. *Nature* **434:** 864–870.

Berger AB, Decourty L, Badis G, Nehrbass U, Jacquier A, Gadal O. 2007. Hmo1 is required for TOR-dependent regulation of ribosomal protein gene transcription. *Mol Cell Biol* **27:** 8015–8026.

Blahnik KR, Dou L, O'Geen H, McPhillips T, Xu X, Cao AR, Iyengar S, Nicolet CM, Ludascher B, Korf I, et al. 2010. Sole-Search: an integrated analysis program for peak detection and functional annotation using ChIP-seq data. *Nucleic Acids Res* **38:** e13.

Boulon S, Westman B, Hutten S, Boisvert F, Lamond A. 2010. The nucleolus under stress. *Mol Cell* **40:** 216–227.

Bywater MJ, Poortinga G, Sanij E, Hein N, Peck A, Cullinane C, Wall M, Cluse L, Drygin D, Anderes K, et al. 2012. Inhibition of RNA polymerase I as a therapeutic strategy to promote cancer-specific activation of p53. *Cancer Cell* **22:** 51–65.

Bywater MJ, Pearson RB, McArthur GA, Hannan RD. 2013. Dysregulation of the basal RNA polymerase transcription apparatus in cancer. *Nat Rev Cancer* **13:** 299–314.

Castillo-Davis CI, Mekhedov SL, Hartl DL, Koonin EV, Kondrashov FA. 2002. Selection for short introns in highly expressed genes. *Nat Genet* **31:** 415–418.

Cavanaugh A, Hirschler-Laszkiewicz I, Rothblum L. 2003. Ribosomal DNA transcription in mammals. In *The Nucleolus* (ed. Olson MOJ), pp. 89–129. Kluwer Academic/Plenum, New York.

Chan JC, Hannan KM, Riddell K, Ng PY, Peck A, Lee RS, Hung S, Astle MV, Bywater M, Wall M, et al. 2011. AKT promotes rRNA synthesis and cooperates with c-MYC to stimulate ribosome biogenesis in cancer. *Sci Signal* **4:** ra56.

Chauvin C, Koka V, Nouschi A, Mieulet V, Hoareau-Aveilla C, Dreazen A, Cagnard N, Carpentier W, Kiss T, Meyuhas O, et al. 2014. Ribosomal protein S6 kinase activity controls the ribosome biogenesis transcriptional program. *Oncogene* **33:** 474–483.

Clemente-Ruiz M, Prado F. 2009. Chromatin assembly controls replication fork stability. *EMBO Rep* **10:** 790–796.

Deisenroth C, Zhang Y. 2010. Ribosome biogenesis surveillance: probing the ribosomal protein-Mdm2-p53 pathway. *Oncogene* **29:** 4253–4260.

Diesch J, Hannan RD, Sanij E. 2014. Perturbations at the ribosomal genes loci are at the centre of cellular dysfunction and human disease. *Cell Biosci* **4:** 43.

Drygin D, Lin A, Bliesath J, Ho CB, O'Brien SE, Proffitt C, Omori M, Haddach M, Schwaebe MK, Siddiqui-Jain A, et al. 2011. Targeting RNA polymerase I with an oral small molecule CX-5461 inhibits ribosomal RNA synthesis and solid tumor growth. *Cancer Res* **71:** 1418–1430.

Drygin D, O'Brien SE, Hannan RD, McArthur GA, Von Hoff DD. 2014. Targeting the nucleolus for cancer-specific activation of p53. *Drug Discov Today* **19:** 259–265.

Elenbaas B, Spirio L, Koerner F, Fleming MD, Zimonjic DB, Donaher JL, Popescu NC, Hahn WC, Weinberg RA. 2001. Human breast cancer cells generated by oncogenic transformation of primary mammary epithelial cells. *Genes Dev* **15:** 50–65.

Fenech M. 2006. Cytokinesis-block micronucleus assay evolves into a "cytome" assay of chromosomal instability, mitotic dysfunction and cell death. *Mutat Res* **600:** 58–66.

Fuda NJ, Ardehali MB, Lis JT. 2009. Defining mechanisms that regulate RNA polymerase II transcription in vivo. *Nature* **461:** 186–192.

Gentleman RC, Carey VJ, Bates DM, Bolstad B, Dettling M, Dudoit S, Ellis B, Gautier L, Ge Y, Gentry J, et al. 2004. Bioconductor: open software development for computational biology and bioinformatics. *Genome Biol* **5:** R80.

Grob A, Colleran C, McStay B. 2014. Construction of synthetic nucleoli in human cells reveals how a major functional nuclear domain is formed and propagated through cell division. *Genes Dev* **28:** 220–230.

Grueneberg DA, Pablo L, Hu KQ, August P, Weng Z, Papkoff J. 2003. A functional screen in human cells identifies UBF2 as an RNA polymerase II transcription factor that enhances the β-catenin signaling pathway. *Mol Cell Biol* **23:** 3936–3950.

Grummt I. 1999. Regulation of mammalian ribosomal gene transcription by RNA polymerase I. *Prog Nucleic Acid Res Mol Biol* **62:** 109–154.

Gunjan A, Paik J, Verreault A. 2005. Regulation of histone synthesis and nucleosome assembly. *Biochimie* **87:** 625–635.

Hamdane N, Stefanovsky VY, Tremblay MG, Nemeth A, Paquet E, Lessard F, Sanij E, Hannan R, Moss T. 2014. Conditional inactivation of Upstream Binding Factor reveals its epigenetic functions and the existence of a somatic nucleolar precursor body. *PLoS Genet* **10:** e1004505.

Han M, Chang M, Kim UJ, Grunstein M. 1987. Histone H2B repression causes cell-cycle-specific arrest in yeast: effects on chromosomal segregation, replication, and transcription. *Cell* **48:** 589–597.

Hannan RD, Rothblum LI. 1995. Regulation of ribosomal DNA transcription during neonatal cardiomyocyte hypertrophy. *Cardiovasc Res* **30:** 501–510.

Hannan R, Stefanovsky V, Arino T, Rothblum L, Moss T. 1999. Cellular regulation of ribosomal DNA transcription: both rat and *Xenopus* UBF1 stimulate rDNA transcription in 3T3 fibroblasts. *Nucleic Acids Res* **27:** 1205–1213.

Hannan KM, Sanij E, Hein N, Hannan RD, Pearson RB. 2011. Signaling to the ribosome in cancer—it is more than just mTORC1. *IUBMB Life* **63:** 79–85.

Hannan KM, Sanij E, Rothblum LI, Hannan RD, Pearson RB. 2013. Dysregulation of RNA polymerase I transcription during disease. *Biochim Biophys Acta* **1829:** 342–360.

Hein N, Sanij E, Quin J, Hannan KM, Ganley ARD, Hannan RD. 2012. The nucleolus and ribosomal genes in aging and senescence. In *Senescence* (ed. Nagata T). InTech, Rijeka, Croatia. http://www.intechopen.com/books/senescence/the-nucleolus-in-aging-and-senescence-.

Hein N, Hannan KM, George AJ, Sanij E, Hannan RD. 2013. The nucleolus: an emerging target for cancer therapy. *Trends Mol Med* **19:** 643–654.

Hovhannisyan H, Cho B, Mitra P, Montecino M, Stein GS, Van Wijnen AJ, Stein JL. 2003. Maintenance of open chromatin and selective genomic occupancy at the cell cycle-regulated histone H4 promoter during differentiation of HL-60 promyelocytic leukemia cells. *Mol Cell Biol* **23:** 1460–1469.

Irizarry RA, Bolstad BM, Collin F, Cope LM, Hobbs B, Speed TP. 2003. Summaries of Affymetrix GeneChip probe level data. *Nucleic Acids Res* **31:** e15.

Laferte A, Favry E, Sentenac A, Riva M, Carles C, Chedin S. 2006. The transcriptional activity of RNA polymerase I is a key determinant for the level of all ribosome components. *Genes Dev* **20:** 2030–2040.

Larson DE, Xie W, Glibetic M, O'Mahony D, Sells BH, Rothblum LI. 1993. Coordinated decreases in rRNA gene transcription factors and rRNA synthesis during muscle cell differentiation. *Proc Natl Acad Sci* **90:** 7933–7936.

Li H, Durbin R. 2009. Fast and accurate short read alignment with Burrows-Wheeler transform. *Bioinformatics* **25:** 1754–1760.

Mais C, Wright JE, Prieto JL, Raggett SL, McStay B. 2005. UBF-binding site arrays form pseudo-NORs and sequester the RNA polymerase I transcription machinery. *Genes Dev* **19:** 50–64.

Marzluff WF, Gongidi P, Woods KR, Jin J, Maltais LJ. 2002. The human and mouse replication-dependent histone genes. *Genomics* **80:** 487–498.

Marzluff WF, Wagner EJ, Duronio RJ. 2008. Metabolism and regulation of canonical histone mRNAs: life without a poly(A) tail. *Nat Rev Genet* **9:** 843–854.

McLean CY, Bristor D, Hiller M, Clarke SL, Schaar BT, Lowe CB, Wenger AM, Bejerano G. 2010. GREAT improves functional interpretation of *cis*-regulatory regions. *Nat Biotechnol* **28:** 495–501.

McStay B, Grummt I. 2008. The epigenetics of rRNA genes: from molecular to chromosome biology. *Annu Rev Cell Dev Biol* **24:** 131–157.

Medina R, Ghule PN, Cruzat F, Barutcu AR, Montecino M, Stein JL, van Wijnen AJ, Stein GS. 2012. Epigenetic control of cell cycle-dependent

histone gene expression is a principal component of the abbreviated pluripotent cell cycle. *Mol Cell Biol* **32:** 3860–3871.

Meeks-Wagner D, Hartwell LH. 1986. Normal stoichiometry of histone dimer sets is necessary for high fidelity of mitotic chromosome transmission. *Cell* **44:** 43–52.

Mendoza-Parra MA, Pattabhiraman S, Gronemeyer H. 2012. Sequential chromatin immunoprecipitation protocol for global analysis through massive parallel sequencing (reChIP-seq). *Protoc Exch* doi: 10.1038/protex.2011.257.

Moss T, Stefanovsky VY. 2002. At the center of eukaryotic life. *Cell* **109:** 545–548.

Moss T, Langlois F, Gagnon-Kugler T, Stefanovsky V. 2007. A housekeeper with power of attorney: the rRNA genes in ribosome biogenesis. *Cell Mol Life Sci* **64:** 29–49.

Myung K, Pennaneach V, Kats ES, Kolodner RD. 2003. *Saccharomyces cerevisiae* chromatin-assembly factors that act during DNA replication function in the maintenance of genome stability. *Proc Natl Acad Sci* **100:** 6640–6645.

Naughton C, Avlonitis N, Corless S, Prendergast JG, Mati IK, Eijk PP, Cockroft SL, Bradley M, Ylstra B, Gilbert N. 2013. Transcription forms and remodels supercoiling domains unfolding large-scale chromatin structures. *Nat Struct Mol Biol* **20:** 387–395.

O'Sullivan AC, Sullivan GJ, McStay B. 2002. UBF binding in vivo is not restricted to regulatory sequences within the vertebrate ribosomal DNA repeat. *Mol Cell Biol* **22:** 657–668.

Phatnani HP, Greenleaf AL. 2006. Phosphorylation and functions of the RNA polymerase II CTD. *Genes Dev* **20:** 2922–2936.

Pinto I, Winston F. 2000. Histone H2A is required for normal centromere function in *Saccharomyces cerevisiae*. *EMBO J* **19:** 1598–1612.

Poortinga G, Hannan KM, Snelling H, Walkley CR, Jenkins A, Sharkey K, Wall M, Brandenburger Y, Palatsides M, Pearson RB, et al. 2004. MAD1 and c-MYC regulate UBF and rDNA transcription during granulocyte differentiation. *EMBO J* **23:** 3325–3335.

Poortinga G, Wall M, Sanij E, Siwicki K, Ellul J, Brown D, Holloway TP, Hannan RD, McArthur GA. 2011. c-MYC coordinately regulates ribosomal gene chromatin remodeling and Pol I availability during granulocyte differentiation. *Nucleic Acids Res* **39:** 3267–3281.

Poortinga G, Quinn LM, Hannan RD. 2014. Targeting RNA polymerase I to treat MYC-driven cancer. *Oncogene* doi: 10.1038/onc.2014.13.

Prado F, Aguilera A. 2005. Partial depletion of histone H4 increases homologous recombination-mediated genetic instability. *Mol Cell Biol* **25:** 1526–1536.

Rao S, Procko E, Shannon MF. 2001. Chromatin remodeling, measured by a novel real-time polymerase chain reaction assay, across the proximal promoter region of the IL-2 gene. *J Immunol* **167:** 4494–4503.

Sanij E, Hannan RD. 2009. The role of UBF in regulating the structure and dynamics of transcriptionally active rDNA chromatin. *Epigenetics* **4:** 374–382.

Sanij E, Poortinga G, Sharkey K, Hung S, Holloway TP, Quin J, Robb E, Wong LH, Thomas WG, Stefanovsky V, et al. 2008. UBF levels determine the number of active ribosomal RNA genes in mammals. *J Cell Biol* **183:** 1259–1274.

Smyth G. 2005. Limma: linear models for microarray data. In *Bioinformatics and computational biology solutions using R and Bioconductor* (ed. Gentleman R, et al.), pp. 397–420. Springer, New York.

Stefanovsky VY, Moss T. 2008. The splice variants of UBF differentially regulate RNA polymerase I transcription elongation in response to ERK phosphorylation. *Nucleic Acids Res* **36:** 5093–5101.

Stefanovsky VY, Pelletier G, Bazett-Jones DP, Crane-Robinson C, Moss T. 2001. DNA looping in the RNA polymerase I enhancesome is the result of non-cooperative in-phase bending by two UBF molecules. *Nucleic Acids Res* **29:** 3241–3247.

Stefanovsky V, Langlois F, Gagnon-Kugler T, Rothblum LI, Moss T. 2006. Growth factor signaling regulates elongation of RNA polymerase I transcription in mammals via UBF phosphorylation and r-chromatin remodeling. *Mol Cell* **21:** 629–639.

White RJ. 2008. RNA polymerases I and III, non-coding RNAs and cancer. *Trends Genet* **24:** 622–629.

Ye X, Franco AA, Santos H, Nelson DM, Kaufman PD, Adams PD. 2003. Defective S phase chromatin assembly causes DNA damage, activation of the S phase checkpoint, and S phase arrest. *Mol Cell* **11:** 341–351.

Zentner GE, Saiakhova A, Manaenkov P, Adams MD, Scacheri PC. 2011. Integrative genomic analysis of human ribosomal DNA. *Nucleic Acids Res* **39:** 4949–4960.

Zhang Y, Liu T, Meyer CA, Eeckhoute J, Johnson DS, Bernstein BE, Nussbaum C, Myers RM, Brown M, Li W, et al. 2008. Model-based analysis of ChIP-Seq (MACS). *Genome Biol* **9:** R137.

Zhu LJ, Pages H, Gazin C, Lawson N, Lin S, Lapointe D, Green M. 2009. *ChIPpeakAnno: Batch annotation of the peaks identified from either ChIP-seq or ChIP-chip experiments.* R package version 1.6.0.